Jurnal Teknologi

Full Paper

ANALYSIS OF ACTIVE SECONDARY SUSPENSION WITH MODIFIED SKYHOOK CONTROLLER TO IMPROVE RIDE PERFORMANCE OF RAILWAY VEHICLE

Fathiah Mohamed Jamil[a], Mohd Azman Abdullah[a,b]*, Mohd Hanif Harun[a,b], Munaliza Ibrahim[a], Fauzi Ahmad[a,b], Ubaidillah Ubaidillah[c]

[a]Fakulti Kejuruteraan Mekanikal, Universiti Teknikal Malaysia Melaka, Hang Tuah Jaya, 76100 Durian Tunggal, Melaka, Malaysia
[b]Centre for Advanced Research on Energy (CARe), Universiti Teknikal Malaysia Melaka, 76100 Durian Tunggal, Melaka, Malaysia
[c]Mechanical Engineering Department, Universitas Sebelas Maret, J1. Ir. Sutami 36A, Kentigan, Sukarta 57126, Indonesia

Article history
Received
31 January 2023
Received in revised form
9 April 2023
Accepted
19 June 2023
Published Online
21 August 2023

*Corresponding author
mohdazman@utem.edu.my

Graphical abstract

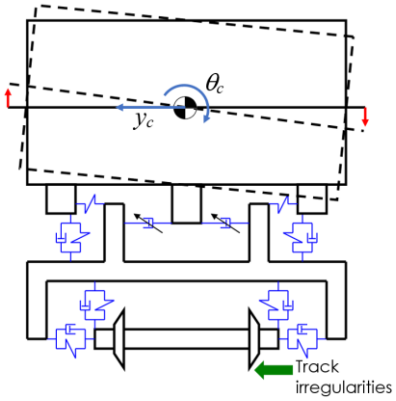

Abstract

The aim of this work is to determine the effectiveness of active suspension control systems in improving the ride quality of railway vehicles. A 13-degrees-of-freedom (DOF) full-body model is provided, including lateral, yaw, and rool motions of the body and bogies, and lateral displacement of the four wheelsets. The suspension system of railway vehicles and the dynamics of track irregularities are combined in a set of governing equations. MATLAB/Simulink is used to build a full-body dynamics model of a rail vehicle. The effectiveness of the active suspension systems equipped with the suggested controller has been tested for the purpose of evaluating its performance. Compared to passive systems, the results showed a more than 60 % improvement in vehicle performance on irregular tracks.

Keywords: Railway vehicle dynamic, active suspension system, modified-skyhook, ride performance, lateral motion

Abstrak

Matlamat kerja ini adalah untuk menentukan keberkesanan sistem kawalan penggantungan aktif dalam meningkatkan kualiti perjalanan kenderaan kereta api. Model badan penuh 13 darjah kebebasan (DOF) disediakan, termasuk gerakan sisi, yaw, dan guling badan dan bogie, dan anjakan sisi empat set roda. Sistem penggantungan kenderaan kereta api dan dinamik ketidakrataan landasan digabungkan dalam satu set persamaan yang mengawal. MATLAB/Simulink digunakan untuk membina model dinamik badan penuh bagi kenderaan kereta api. Keberkesanan sistem penggantungan aktif yang dilengkapi dengan pengawal cadangan telah diuji untuk tujuan menilai prestasinya. Berbanding dengan sistem pasif, keputusan menunjukkan peningkatan lebih daripada 60 % dalam prestasi kenderaan pada landasan yang tidak rata.

Kata kunci: Dinamik kenderaan kereta api, sistem penggantungan aktif, cangkuk-langit diubahsuai, prestasi tunggangan, gerakan sisi

1.0 INTRODUCTION

As high-speed railway vehicles have proven to be an efficient and less expensive mode of transport, numerous governments have expressed interest in their development. At high speeds, however, important things like riding comfort or safety deteriorate, which in the worst case can lead to bad things like a railway vehicle derailment. The high speed would generate large body vibrations in the railway vehicle, leading to problems with running stability and ride quality [1] and maintenance costs [2]. Therefore, in order to make railway vehicles more comfortable and safer, it is necessary to reduce vibration and reduce the swaying phenomenon in the car body [3]. In addition, an untuned suspension system with a state-of-the-art engine can significantly affect ride comfort or possibly lead to fatalities, making suspension system one of the most important technologies in railway vehicles [3].

In general, the vehicle's suspension system is the key to the safety and comfort of passengers, as it effectively isolates the body from ground-induced vibrations [4]. The damper should convert vibration energy into heat and absorb the vibrations caused by the unevenness of the ground surface [5, 6]. There are three distinct categories of suspension systems, known respectively as passive, semi-active and active [7]. Compared to the traditional passive approach, semi-active suspension technology in railway vehicles offers higher opportunities to improve their dynamic performances [8, 9, 10]. The use of springs and pneumatics in active railway vehicle suspension systems offers several advantages, including simplifying the overall vehicle design and reducing operating costs [11, 12]. When active control is being applied to a railway vehicle's secondary suspensions, the ride quality is improved, making it more comfortable to ride [13, 14]. In addition, an active suspension system also has the ability to generate energy that can be used to create relative motion between the body and the wheelsets that dynamically responds to changes in the track profiles [15, 16]. However, to do so, they require a significant amount of power and a complex control implementation. In addition, evaluating the stability of the control system is important, as railway vehicles on the track could gain or retain more mechanical performance through the use of active suspension technologies [17, 18]. Active control can be used with both lateral and vertical secondary suspensions aimed at reacting to track irregularities [15, 17]. Active suspension innovation with sensors sensing important variables such as displacement, speed, acceleration and pressure aid in the development of an actuation controller, resulting in a comfortable ride within the allowable deflection range [13, 18].

Railway vehicle suspension systems consist of sensors, actuators, and the force required for actuators is been controlled by a specific law to produce the desired force. Therefore, the appropriate control must be implemented to generate the force required by the systems. Control strategy is the hub of system control and has a significant impact on how efficiently an active control system operates. Due to the potential benefits of active control, which includes sensors, actuators and electronic controls to create an active suspension system, its implementation in railway vehicle suspension systems is under investigation [19].

In the previous study, a variety of control systems aimed at improving the performance of railway vehicles were presented, such as an LQR controller [20], fuzzy logic [21, 22], sliding mode [23] and magnetorheological damper [24, 25, 26], which helps to reduce the vibration of the moving body. Skyhook theory has been extensively researched for its application in automotive and railway vehicle systems as a means of providing suspension control [27, 28]. Based on literature reviews, it can concluded that the skyhook control law can make railway vehicles more comfortable on long journeys [29, 30]. This regulatory framework was first proposed in 1974 [31]. The Skyhook damper provides damping without transmitting unsprung mass vibrations to the body because it is not attached to the unsprung mass. For this reason, the damper is segmented in such a way that the damping force is proportional to the absolute speed of the sprung masses [31].

In this paper, the effects of a modified skyhook controller on railway vehicle ride performance were determined through active secondary suspensions. In the first stage, a full 13-DOF railway dynamics mathematical model was developed. In the second stage, the railway dynamics model was then simulated and analyzed using MATLAB/Simulink. In the final stage, the proposed control system was implemented on the model. Reductions in vibrations were observed at subsequently the reductions represented the improvement in ride performance of the railway vehicle.

2.0 METHODOLOGY

2.1 Dynamic Mathematical Modelling of Railway Vehicle

The model for railway dynamic systems is derived mathematically using Newton's second law [X8]. The suspension components placed between the vehicle body and the bogies are modeled as the secondary system, while the suspension components placed between the bogie and the wheelsets are modeled as the primary suspension. In this study, a 13-degree-of-freedom model is developed to study the motions of the body, bogie, and wheelsets of a train. Figure 1, Figure 2 and Figure 3 show the arrangement of the railway vehicle with its suspensions.

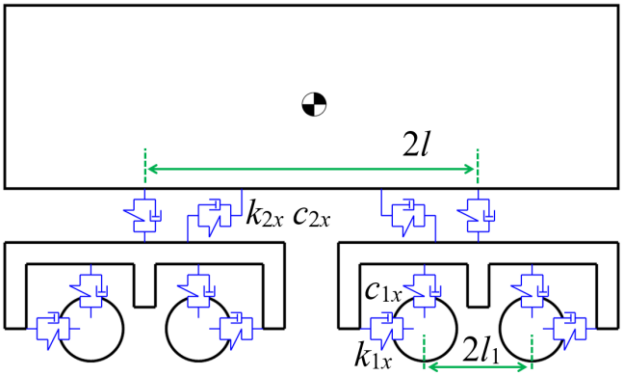

Figure 1 Side view

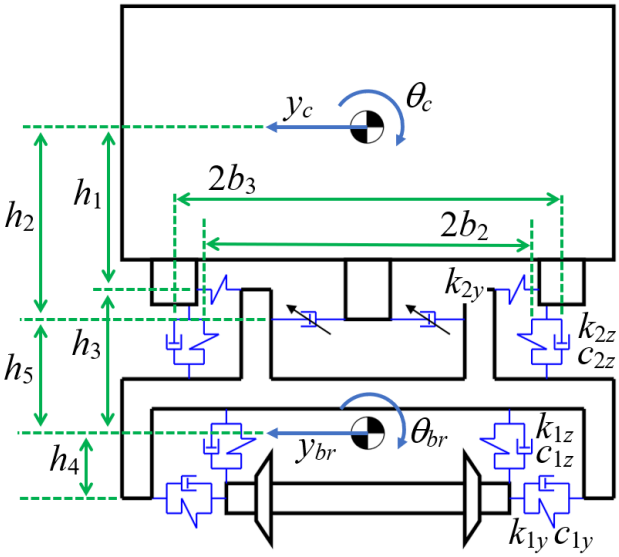

Figure 2 Rear View

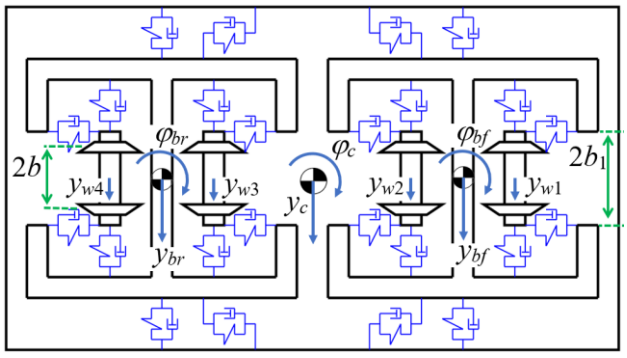

Figure 3 Top View

The 13-DOF mathematical equations are presented in Equation (1) to Equation (13). All the symbols for the parameters are tabulated in Table 1. The variables and equations' states are described in Table 2.

i. Car Body Dynamics

The lateral force due to the car body mass is represented by:

$$\begin{aligned} m_c\ddot{y}_c = &-k_{2y}(y_c + l\varphi_c - h_1\theta_c - y_{bf} \\ &- h_3\theta_{bf} - c_{2y}(\dot{y}_c + l\dot{\varphi}_c \\ &- h_2\dot{\theta}_c - \dot{y}_{bf} - h_5\dot{\theta}_{bf}) \\ &- k_{2y}(y_c - l\varphi_c - h_1\theta_c \\ &- y_{br} - h_3\theta_{br}) - c_{2y}(\dot{y}_c \\ &- l\dot{\varphi}_c - h_2\dot{\theta}_c - \dot{y}_{br} \\ &- h_5\dot{\theta}_{br}) \end{aligned} \quad (1)$$

The yawing and rolling moments of the car body can be described by the following equations:

$$\begin{aligned} I_{cz}\ddot{\varphi}_c = &-k_{2y}l(y_c + l\varphi_c - h_1\theta_c - y_{bf} \\ &- h_3\theta_{bf}) \\ &- c_{2y}l(\dot{y}_c + l\dot{\varphi}_c - h_2\dot{\theta}_c \\ &- \dot{y}_{bf} - h_5\dot{\theta}_{bf}) \\ &+ k_{2y}l(y_c - l\varphi_c - h_1\theta_c \\ &- y_{br} - h_3\theta_{br}) \\ &+ c_{2y}l(\dot{y}_c l\dot{\varphi}_c - h_2\dot{\theta}_c \\ &- \dot{y}_{br} - h_5\dot{\theta}_{br}) \\ &- k_{2x}{b_2}^2(\varphi_c \\ &- \varphi_{bf}) - c_{2x}{b_3}^2(\dot{\varphi}_c \\ &- \dot{\varphi}_{bf}) \\ &+ k_{2x}{b_2}^2(\varphi_c - \varphi_{br}) \\ &- c_{2x}{b_3}^2(\dot{\varphi}_c - \dot{\varphi}_{br}) \end{aligned} \quad (2)$$

$$\begin{aligned} I_{cx}\ddot{\theta}_c = &-k_{2y}h_1(y_c + l\varphi_c - h_1\theta_c - y_{bf} \\ &- h_3\theta_{bf}) \\ &+ c_{2y}h_2(\dot{y}_c + l\dot{\varphi}_c - h_2\dot{\theta}_c \\ &- \dot{y}_{bf} - h_5\dot{\theta}_{bf}) \\ &+ k_{2y}h_1(y_c - l\varphi_c - h_1\theta_c \\ &- y_{br} - h_3\theta_{br}) \\ &+ c_{2y}h_2(\dot{y}_c - l\dot{\varphi}_c - h_2\dot{\theta}_c \\ &- \dot{y}_{br} - h_5\dot{\theta}_{br}) \\ &- k_{2x}{b_2}^2(\theta_c - \theta_{bf}) \\ &- c_{2x}{b_3}^2(\dot{\theta}_c - \dot{\theta}_{bf}) \\ &+ k_{2x}{b_2}^2(\theta_c - \theta_{br}) \\ &- c_{2x}{b_3}^2(\dot{\theta}_c - \dot{\theta}_{br}) \end{aligned} \quad (3)$$

ii. Bogie Dynamics

The lateral forces due to the front and rear bogies' mass are represented by:

$$\begin{aligned} m_b\ddot{y}_{bf} = &\ k_{2y}(y_c - l\varphi_c - h_2\theta_c y_{bf} - h_3\theta_{bf}) \\ &+ c_{2y}(\dot{y}_c - l\dot{\varphi}_c - h_2\dot{\theta}_c\dot{y}_{bf} \\ &- h_5\dot{\theta}_{bf}) - k_{1y}(y_{bf} \\ &- l_1\varphi_{bf} - h_4\theta_{bf} - y_{w1}) \\ &- c_{1y}(\dot{y}_{bf} - l_1\dot{\varphi_{bf}} \\ &- h_4\dot{\theta}_{bf} - \dot{y}_{w1}) - k_{1y}(y_{bf} \\ &- l_1\varphi_{bf} - h_4\theta_{bf} - y_{w2}) \\ &- c_{1y}(\dot{y}_{bf} - l_1\dot{\varphi_{bf}} \\ &- h_4\dot{\theta}_{bf} - \dot{y}_{w2}) \end{aligned} \quad (4)$$

$$
\begin{aligned}
m_b\ddot{y}_{br} = {} & k_{2y}(y_c + l\varphi_c - h_1\theta_c y_{br} - h_3\theta_{br}) \\
& + c_{2y}(\dot{y}_c + l\dot{\varphi}_c - h_2\dot{\theta}_c\dot{y}_{br} \\
& - h_5\dot{\theta}_{br}) - k_{1y}(y_{br} \\
& - l_1\varphi_{br} - h_4\theta_{br} - y_{w3}) \\
& - c_{1y}(\dot{y}_{br} - l_1\dot{\varphi_{br}} \\
& - h_4\dot{\theta}_{br} - \dot{y}_{w3}) \\
& - k_{1y}(y_{br} - l_1\varphi_{br} \\
& - h_4\theta_{br} - y_{w4}) \\
& - c_{1y}\left(\dot{y}_{br} - l_1\dot{\varphi_{br}}\right. \\
& \left. - h_4\dot{\theta}_{br} - \dot{y}_{w4}\right)
\end{aligned} \tag{5}
$$

The yawing moments of the front and rear bogies are described by the following equations:

$$
\begin{aligned}
I_{bz}\ddot{\varphi}_{br} = {} & k_{2x}\,{b_2}^2(\varphi_c - \varphi_{br}) \\
& + c_{2x}\,{b_3}^2(\dot{\varphi}_c \\
& - \dot{\varphi}_{br}) - k_{1y}\,l_1(y_{br} \\
& + l_1\varphi_{br} - h_4\theta_{br} \\
& - y_{w3}) - c_{1y}l_1(\dot{y}_{br} \\
& + l_1\dot{\varphi}_{br} - h_4\dot{\theta}_{br} - \dot{y}_{w3}) \\
& + k_{1y}\,l_1(y_{br} + l_1\varphi_{br} \\
& - h_4\theta_{br} - y_{w4}) \\
& + c_{1y}l_1\left(\dot{y}_{br} + l_1\dot{\varphi}_{br}\right. \\
& \left. - h_4\dot{\theta}_{br} - \dot{y}_{w4}\right) \\
& - k_{1x}\,{b_1}^2(\varphi_{br} - \varphi_{w3}) \\
& - c_{1x}\,{b_1}^2(\dot{\varphi}_{br} - \dot{\varphi}_{w3}) \\
& - k_{1x}\,{b_1}^2(\varphi_{br} - \varphi_{w4}) \\
& - c_{1x}\,{b_1}^2(\dot{\varphi}_{br} - \dot{\varphi}_{w4})
\end{aligned} \tag{6}
$$

$$
\begin{aligned}
I_{bz}\ddot{\varphi}_{bf} = {} & k_{2x}\,{b_2}^2(\varphi_c - \varphi_{bf}) \\
& - c_{2x}\,{b_3}^2(\dot{\varphi}_c - \dot{\varphi}_{bf}) \\
& - k_{1y}\,l_1(y_{bf} + l_1\varphi_{bf} \\
& - h_4\theta_{bf} - y_{w1}) \\
& - c_{1y}l_1(\dot{y}_{bf} + l_1\dot{\varphi}_{bf} \\
& - h_4\dot{\theta}_{bf} - \dot{y}_{w1}) \\
& + k_{1y}\,l_1(y_{bf} + l_1\varphi_{bf} \\
& - h_4\theta_{bf} - y_{w2}) \\
& + c_{1y}l_1(\dot{y}_{bf} + l_1\dot{\varphi}_{bf} \\
& - h_4\dot{\theta}_{bf} - \dot{y}_{w2}) \\
& - k_{1x}\,{b_1}^2(\varphi_{bf} - \varphi_{w1}) \\
& - c_{1x}\,{b_1}^2(\dot{\varphi}_{bf} - \dot{\varphi}_{w1}) \\
& - k_{1x}\,{b_1}^2(\varphi_{bf} - \varphi_{w2}) \\
& - c_{1x}\,{b_1}^2(\dot{\varphi}_{bf} - \dot{\varphi}_{w2})
\end{aligned} \tag{7}
$$

EqUation (8) and (9) show the rolling moments of the front and rear bogies respectively.

$$
\begin{aligned}
I_{bx}\ddot{\theta}_{bf} = {} & -k_{2y}h_3(y_c + l\varphi_c - h_1\theta_c \\
& - y_{bf} - h_3\theta_{bf}) \\
& + c_{2y}h_5(\dot{y}_c + l\dot{\varphi}_c - h_2\dot{\theta}_c \\
& - \dot{y}_{bf} - h_5\dot{\theta}_{bf}) \\
& + k_{2z}\,{b_2}^2(\theta_c - \theta_{bf}) \\
& + c_{2z}\,{b_3}^2(\dot{\theta}_c - \dot{\theta}_{bf}) \\
& + c_{1y}h_4(\dot{y}_{bf} + l_1\dot{\varphi_{bf}} \\
& - h_4\dot{\theta}_{bf} - \dot{y}_{w1}) \\
& + k_{1y}h_4(y_{bf} - l_1\varphi_{bf} \\
& - h_4\theta_{bf} - y_{w2})) \\
& + c_{1y}\,h_4(\dot{y}_{bf} - l_1\dot{\varphi_{bf}} \\
& - h_4\dot{\theta}_{bf} - \dot{y}_{w2}) \\
& - 2c_{1z}\,{b_1}^2\theta_{bf} \\
& - 2k_{1z}\,{b_1}^2\dot{\theta}_{bf}
\end{aligned} \tag{8}
$$

$$
\begin{aligned}
I_{bx}\ddot{\theta}_{br} = {} & k_{2y}h_3(y_c - l\varphi_c - h_1\theta_c \\
& - y_{br} - h_3\theta_{br}) + c_{2y}h_5\,(\dot{y}_c \\
& - l\dot{\varphi}_c - h_2\dot{\theta}_c - \dot{y}_{br} \\
& - h_5\dot{\theta}_{br}) \\
& + k_{2z}\,{b_2}^2(\theta_c - \theta_{br}) \\
& + c_{2z}\,{b_3}^2(\dot{\theta}_c - \dot{\theta}_{br}) \\
& + k_{1y}h_4(y_{br} + l_1\varphi_{br} \\
& - h_4\theta_{br} - y_{w3}) \\
& + + c_{1y}h_4\,(\dot{y}_{br} + l_1\dot{\varphi_{br}} \\
& - \quad h_4\dot{\theta}_{br} - \dot{y}_{w3}) \\
& + k_{1y}h_4(y_{br} - l_1\varphi_{br} \\
& - h_4\theta_{br} - y_{w4}) \\
& + c_{1y}\,h_4(\dot{y}_{br} - l_1\dot{\varphi}_{br} \\
& - h_4\dot{\theta}_{br} - \dot{y}_{w4}) \\
& - 2k_{1z}\,{b_1}^2\theta_{br} \\
& - 2c_{1z}\,{b_1}^2\dot{\theta}_{br}
\end{aligned} \tag{9}
$$

iii. Wheelset Dynamics

There are four sets of wheels; 1st and 2nd wheelsets are at the front bogie and 3rd and 4th wheelsets are at the rear bogie. The lateral forces due to the wheelsets' masses are denoted by:

$$
\begin{aligned}
m_w\ddot{y}_{w1} = {} & k_{1y}(y_{bf} + l_1\varphi_{bf} - h_4\theta_{bf} - y_{w1}) \\
& + c_{1y}\,(\dot{y}_{bf} + l_1\dot{\varphi_{bf}} \\
& - h_4\dot{\theta}_{bf} - \dot{y}_{w1}) \\
& - 2f_{22}\left[\frac{\dot{y}_{w1}}{V}\left(1 + \frac{\sigma r_0}{b}\right)\right. \\
& \left. - \varphi_{w1}\right] + K_{gy}y_{w1} \\
& - 2f_{22}\left[\frac{\sigma r_0}{V_b}\dot{y}_{a1}\right. \\
& \left. + \frac{\sigma {r_0}^2}{V_b}\,\dot{\theta}_{cl1}\right] + K_{gy}(y_{a1} \\
& + r_0\theta_{cl1})
\end{aligned} \tag{10}
$$

$$m_w\ddot{y}_{w2} = k_{1y}(y_{bf} + l_1\varphi_{bf} - h_4\theta_{bf} - y_{w2}) + c_{1y}\left(\dot{y}_{bf} + l_1\dot{\varphi_{bf}} - h_4\dot{\theta}_{bf} - \dot{y}_{w2}\right) - 2f_{22}\left[\frac{\dot{y}_{w2}}{V}\left(1 + \frac{\sigma r_0}{b}\right) - \varphi_{w2}\right] + K_{gy}y_{w2} - 2f_{22}\left[\frac{\sigma r_0}{V_b}\dot{y}_{a2} + \frac{\sigma {r_0}^2}{V_b}\dot{\theta}_{cl2}\right] + K_{gy}(y_{a2} + r_0\theta_{cl2}) \quad (11)$$

$$m_w\ddot{y}_{w3} = k_{1y}(y_{br} + l_1\varphi_{br} - h_4\theta_{br} - y_{w3}) + c_{1y}\left(\dot{y}_{br} + l_1\dot{\varphi_{br}} - h_4\dot{\theta}_{br} - \dot{y}_{w3}\right) - 2f_{22}\left[\frac{\dot{y}_{w3}}{V}\left(1 + \frac{\sigma r_0}{b}\right) - \varphi_{w3}\right] + K_{gy}y_{w3} - 2f_{22}\left[\frac{\sigma r_0}{V_b}\dot{y}_{a3} + \frac{\sigma {r_0}^2}{V_b}\dot{\theta}_{cl3}\right] + K_{gy}(y_{a3} + r_0\theta_{cl3}) \quad (12)$$

$$m_w\ddot{y}_{w4} = k_{1y}(y_{br} + l_1\varphi_{br} - h_4\theta_{br} - y_{w4}) + c_{1y}\left(\dot{y}_{br} + l_1\dot{\varphi_{br}} - h_4\dot{\theta}_{br} - \dot{y}_{w4}\right) - 2f_{22}\left[\frac{\dot{y}_{w4}}{V}\left(1 + \frac{\sigma r_0}{b}\right) - \varphi_{w4}\right] + K_{gy}y_{w4} - 2f_{22}\left[\frac{\sigma r_0}{V_b}\dot{y}_{a4} + \frac{\sigma {r_0}^2}{V_b}\dot{\theta}_{cl4}\right] + K_{gy}(y_{a4} + r_0\theta_{cl4}) \quad (13)$$

2.2 MATLAB/Simulink & Simulation Model

Figure 4 shows the schematic structure of 13-DOF railway vehicle assembly represented as a block diagram in MATLAB/Simulink by referencing the derived dynamic mathematical model. The simulated assembly includes the vehicle body, bogies and wheelsets, all connected by the spring and damper components of the primary and secondary suspension [X6]. Then the model is simulated to study the performance difference between passive and active secondary suspension. When it comes to technical computing, MATLAB is the language of choice because it integrates programming, computation, and visualization in a single platform [32].

In order to reduce the possibility of errors occurring during the simulation process, the models used in the programmed MATLAB Simulink must fully follow the specified equations. It is assumed that the complexity of the models is reduced, and the number of unknowns is minimized. The assumptions imply that the excitation of the track is transmitted to the car body via the wheelset to the primary suspensions, to the bogies, and secondary suspensions systems. It is permissible for the car body mass and bogies' masses to roll, yaw and move laterally. The wheelsets' masses are considered as a rigid body apart from their ability to move laterally, which is the only direction they can move. Finally, the track irregularities in layout are seen as the external disturbance in the system.

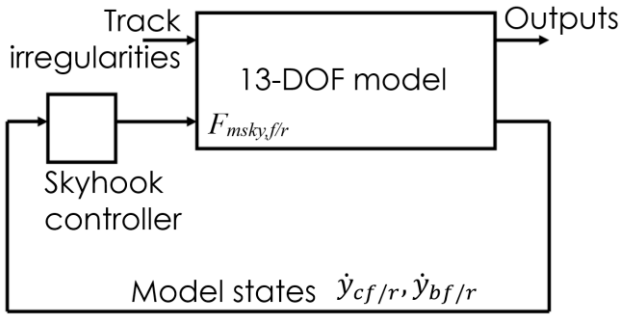

Figure 4 Schematic railway vehicle structure in MATLAB/Simulink

2.3 Modified Skyhook Controller

In this study, Skyhook has been used as the controller because Skyhook was the best suspension controller because it allowed the vehicle to hold its position as if it were hanging from an imaginary hook in the sky, regardless of track conditions [X22]. The Skyhook damping method is positioned between the spring mass and a notional point in the sky. With this controller, passive suspension systems no longer have to choose between resonance control and high-frequency operation [X23]. However, due to an issue caused by the implementation of the original skyhook controller, the skyhook had to be modified to provide the adequate force to mitigate the track irregularities in the simulation [29, 30]. The dynamic equations of the modified Skyhook controller are given as follows:

$$F_{msky,f} = C_{msky,f}[\alpha(\dot{y}_{cf} - \dot{y}_{bf}) + (1 - \alpha)\dot{y}_{bf}] \quad (14)$$

$$F_{msky,r} = C_{msky,r}[\alpha(\dot{y}_{cr} - \dot{y}_{br}) + (1 - \alpha)\dot{y}_{br}] \quad (15)$$

Where $F_{msky,f}$ and $F_{msky,r}$ are the skyhook forces of front and rear dampers, $C_{msky,f}$ and $C_{msky,r}$ are the coefficients of skyhook controller of front and rear damper while α is the ratio of the bogie mass modified skyhook. Figures 5 and 6 shows the block diagram of

modified skyhook controller and schematic diagram of railway suspension with skyhook controller.

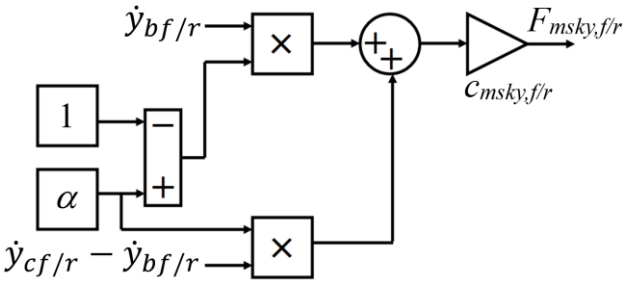

Figure 5 Modified skyhook controller

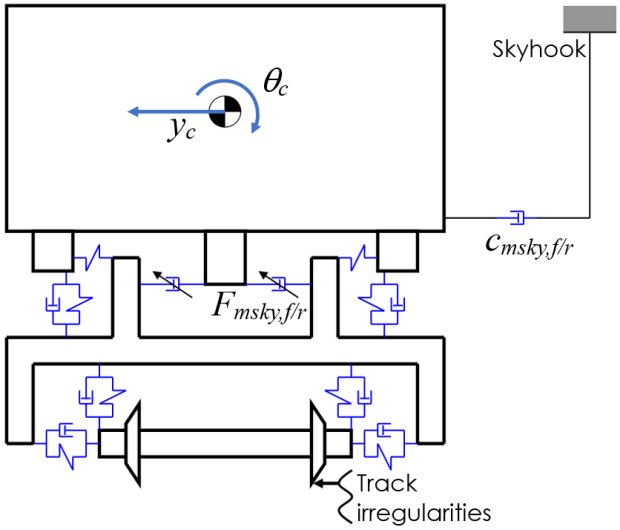

Figure 6 Schematic diagram of railway suspension with skyhook controller

The system inputs are the track random input disturbances with amplitude of 0.01 to - 0.01 m [8, 26]. Sensors are utilized to monitor system outputs such as lateral displacement and yaw angle and transmit measurements to the controller. The controller determines the appropriate amount of control action to be applied to the system, and the actuators carry out this control action.

2.4 Parameters and Equations' States

Table 1 Parameters used in developing the 13-DOF passenger vehicle model [20].

Symbol	Parameters	Value
m_c	Vehicle body mass (kg)	32000
m_b	Vehicle bogie mass (kg)	3296
m_w	Vehicle wheel mass (kg)	1750
k_{1y}	Double of primary lateral stiffness (N/m)	29000000
k_{1x}	Double primary longitudinal stiffness (N/m)	15000000
k_{1z}	Double of primary vertical stiffness (N/m)	1330000
C_{1y}	Double of primary lateral damping (Ns/m)	0
C_{1x}	Double of primary longitudinal damping (Ns/m)	0
C_{1z}	Double of primary vertical damping (Ns/m)	30000
k_{2y}	Double of primary lateral stiffness (N/m)	350000
k_{2x}	Double primary longitudinal stiffness (N/m)	340000
k_{2z}	Double of primary vertical stiffness (N/m)	680000
C_{2y}	Double of primary lateral damping (Ns/m)	52000
C_{2x}	Double of primary longitudinal damping (Ns/m)	500000
C_{2z}	Double of primary vertical damping (Ns/m)	160000
b	Half of wheelset contact distance (m)	0.7465
b_1	Half of primary suspension spacing (lateral) (m)	1
b_2	Half of secondary spring spacing (lateral) (m)	1
b_3	Half of secondary vertical damper spacing (m)	1
I_w	Roll moment of inertia of wheelset (kg.m^2)	1400
I_{bz}	Yaw moment of inertia of bogie (kg.m^2)	2100
I_{bx}	Roll moment of inertia of bogie (kg.m^2)	1900
I_{cz}	Yaw moment of inertia of car body (kg.m^2)	2100
I_{cx}	Roll moment of inertia of car body (kg.m^2)	1900
w	Load per wheelset (N)	1117000
l	Half of bogie centre pin spacing(m)	1.25
l_1	Half of wheelbase (m)	3.5
V	Vehicle speed (km/h)	300

Symbol	Parameters	Value
h_1	Vertical distance from car body centre of gravity to secondary spring (m)	0.763
h_2	Vertical distance from car body centre of gravity to secondary lateral damper (m)	0.78
h_3	Vertical distance from bogie frame centre of gravity to secondary spring (m)	0.0245
h_4	Vertical distance from bogie frame centre of gravity to primary suspension (m)	-0.0285
h_5	Vertical distance from bogie frame centre of gravity to primary suspension (m)	0.2175
r_0	Wheel rolling radius (m)	0.4575
f_{11}	Longitudinal creep coefficient	11200000
f_{22}	Lateral creep coefficient	9980000
λ_e	Effective wheel conicity	0.05
σ	Wheelset roll coefficient	0.05
A_a	Scalar factor of lateral alignment	10.80×10^{-7}
A_v	Scalar factor of cross-level	6.125×10^{-7}

Table 2 Equations' states

State	Description
$\ddot{y}_c$	Lateral acceleration of the railway car body (m/s²)
$\dot{y}_c$	Lateral velocity of the railway car body (m/s)
y_c	Lateral displacement of the railway car body (m)
$\ddot{\varphi}_c$	Yaw angular acceleration of the railway car body (rad/s²)
$\dot{\varphi}_c$	Yaw angular velocity of the railway car body (rad/s)
φ_c	Yaw angular displacement of the railway car body (rad)
$\ddot{\theta}_c$	Roll angular acceleration of the railway car body (rad/s²)
$\dot{\theta}_c$	Roll angular velocity of the railway car body (rad/s)
θ_c	Roll angular displacement of the railway car body (rad)
$\ddot{y}_{bf}$	Lateral acceleration of the front bogie (m/s²)
$\dot{y}_{bf}$	Lateral velocity of the front bogie (m/s)
y_{bf}	Lateral displacement of the front bogie (m)
$\ddot{\varphi}_{bf}$	Yaw angular acceleration of the front bogie (rad/s²)
$\dot{\varphi}_{bf}$	Yaw angular velocity of the front bogie (rad/s)
φ_{bf}	Yaw angular displacement of the front bogie (rad)
$\ddot{\theta}_{bf}$	Roll angular acceleration of the front bogie (rad/s²)
$\dot{\theta}_{bf}$	Roll angular velocity of the front bogie (rad/s)
θ_{bf}	Roll angular displacement of the front bogie (rad)
$\ddot{y}_{br}$	Lateral acceleration of the rear bogie (m/s²)
$\dot{y}_{br}$	Lateral velocity of the rear bogie (m/s)
y_{br}	Lateral displacement of the rear bogie (m)
$\ddot{\varphi}_{br}$	Yaw angular acceleration of the rear bogie (rad/s²)
$\dot{\varphi}_{br}$	Yaw angular velocity of the rear bogie (rad/s)
φ_{br}	Yaw angular displacement of the rear bogie (rad)
$\ddot{\theta}_{br}$	Roll angular acceleration of the rear bogie (rad/s²)
$\dot{\theta}_{br}$	Roll angular velocity of the rear bogie (rad/s)
θ_{br}	Roll angular displacement of the rear bogie (rad)
$\ddot{y}_{w1}$	Lateral acceleration of the 1st wheelset (m/s²)
$\dot{y}_{w1}$	Lateral velocity of the 1st wheelset (m/s)
y_{w1}	Lateral displacement of the 1st wheelset (m)
$\ddot{y}_{w2}$	Lateral acceleration of the 2nd wheelset (m/s²)
$\dot{y}_{w2}$	Lateral velocity of the 2nd wheelset (m/s)
y_{w2}	Lateral displacement of the 2nd wheelset (m)
$\ddot{y}_{w3}$	Lateral acceleration of the 3rd wheelset (m/s²)
$\dot{y}_{w3}$	Lateral velocity of the 3rd wheelset (m/s)

State	Description
y_{w3}	Lateral displacement of the 3rd wheelset (m)
$\ddot{y}_{w4}$	Lateral acceleration of the 4th wheelset (m/s^2)
$\dot{y}_{w4}$	Lateral velocity of the 4th wheelset (m/s)
y_{w4}	Lateral displacement of the 4th wheelset (m)

3.0 RESULTS AND DISCUSSION

In this study, the analysis is performed on a full 13-DOF railway vehicle model through a simulation approach that includes lateral, yaw, and roll displacements and accelerations of the car body. The purpose of this study is to evaluate the dynamic performance of the railway vehicle while moving on the track profile and the car body is excited by the lateral disturbance from the two bogies. Therefore, the performance evaluation was performed by comparing the amplitude values between passive and active suspension with the implementation of a modified skyhook controller in the system.

3.1 Model Verification

The simulation inputs and outputs of the 13-DOF model were compared to the experimental inputs and outputs from previous research [8] for verification. Figure 7 and Figure 8 show the lateral alignment and cross-level inputs respectively. The simulation inputs for lateral alignment and cross-level are randomized at amplitude between -15 to 15 mm and -8 to 8 mm respectively to reproduce the experimental inputs. It is considered acceptable for the simulation inputs since the pattern and range are within amplitudes of the experimental inputs. Figure 9 shows car body the lateral acceleration responses between simulation and experiment. Since the pattern and range of the simulation output are almost match the experimental output, the model is considered verified and can be further used in controller design.

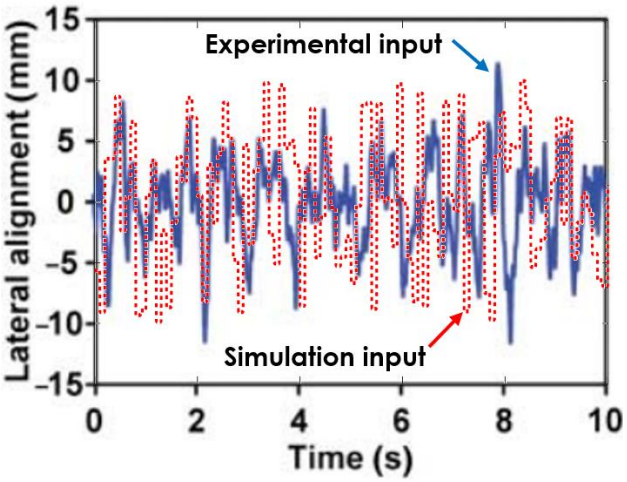

Figure 7 Random input for the simulation compared to the actual experimental input (lateral alignment)

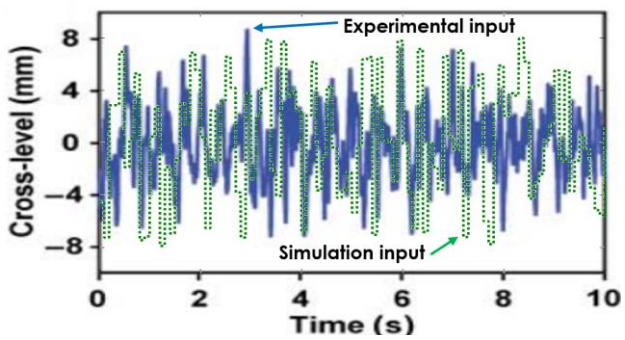

Figure 8 Random input for the simulation compared to the actual experimental input (cross-level)

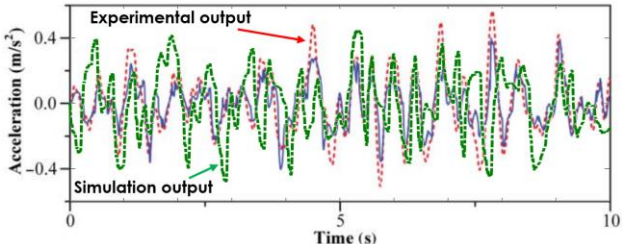

Figure 9 Railway body lateral acceleration outputs comparison between simulation and experiment

3.2 Car Body Displacement

The effectiveness of the active suspension with the modified skyhook controller implementation was observed on the car body's lateral, yaw and roll displacements. Figures 10 to 12 show the controller's response when the random input was applied to the system. As expected, when the modified controller works, a reduction in amplitude compared to passive suspension was obtained. The peak-to-peak values and the root mean square (RMS) values for lateral displacement, yaw and roll angular displacements.

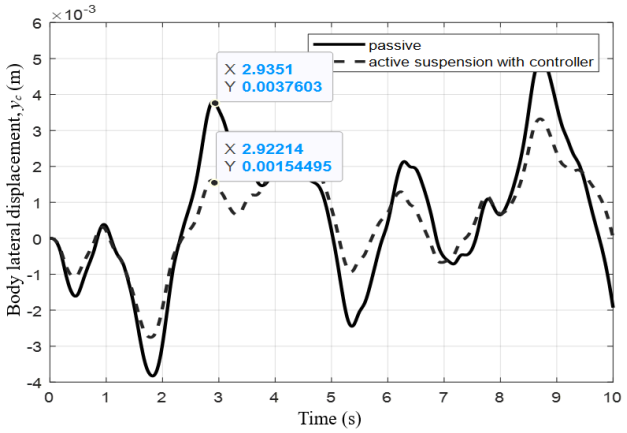

Figure 10 Railway body lateral displacement response for random input disturbance

There are about 5 peaks for the body lateral displacement within time range of 10 s but only 2 peaks show significant values as shown in Figure 10. The effect of modified skyhook controller to the secondary suspension systems helps the car body sway less compared to the passive suspension. One of peak-to-peak value of body displacement for the passive suspension system is 0.0037603 m at 2.9 s, while for the system with modified skyhook controllers have small peak-to-peak values of the body displacement which is 0.00154495 m where the improvement was 58.9 %. It also can be seen from the RMS value where the percentage differences between passive and active was 99.4 % (Table 3).

Table 3 Peak-to-peak and RMS values of lateral body displacement

Car body lateral displacement	y_c (m)	
	Peak to Peak	RMS
Passive suspension	0.0037603	0.001929
Active suspension (Modified skyhook controller)	0.00154495	1.109x10^{-5}
Improvement (%) $= \frac{y_{c,passive} - y_{c,active}}{y_{c,passive}} \times 100\%$	58.9	99.4

When the random inputs applied to the system, the result (Figure 11 and Table 4) shows the unwanted yaw angular displacement percentage of overshoot reduced by almost 76.11 % with 2 peaks show high values, in which, one of them gave the value of 6.73 x 10^{-5} rad/s with modified skyhook controller and 0.000281779rad/s for passive suspension. The RMS value gave the percentage of 82.63 % with the passive suspension value was 0.0002429 rad/s and active suspension was 4.217 x 10^{-5} rad/s.

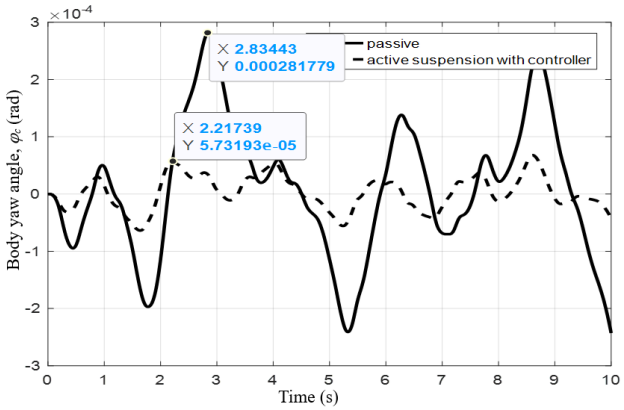

Figure 11 Railway body yaw angular displacement response for random input disturbance

Table 4 peak-to-peak and RMS values of body yaw displacement

Car body yaw	φ_c (rad)	
	Peak to Peak	RMS
Passive suspension	0.000281779	0.0002429
Active suspension (Modified skyhook controller)	6.73x10^{-5}	4.217x10^{-5}
Improvement (%) $= \frac{\varphi_{c,passive} - \varphi_{c,active}}{\varphi_{c,passive}} \times 100\%$	76.11	82.63

For roll angle response (Figure 12), the graph shows an almost consistent pattern of amplitudes, with the peak-to-peak values for passive and modified skyhook are 0.000802927 rad, and 0.000420812 rad respectively. The RMS giving the percentage difference of 58.26% between passive and active as shown in Table 5. Thus, the proposed controller clearly demonstrated its ability to reduce body vibrations in terms of body linear and angular displacements.

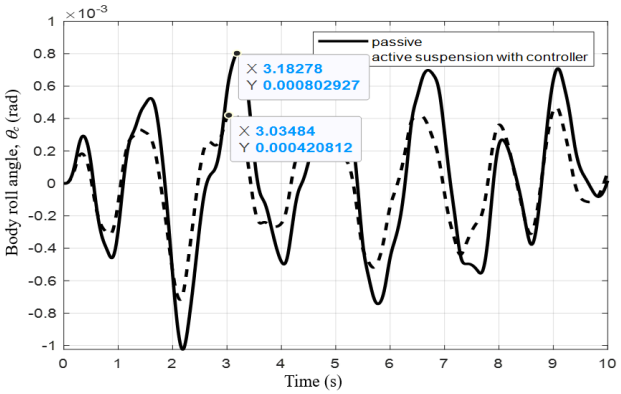

Figure 12 Railway body roll angular displacement response for random input disturbance

Table 5 Peak-to-peak and RMS values of body roll displacement

Car body roll	θ_c(rad)	
	Peak to Peak	RMS
Passive suspension	0.00080292	1.704×10^{-5}
Active suspension (Modifed skyhook controller)	0.00042081	7.111×10^{-6}
Improvement (%) $= \frac{\theta_{c,passive} - \theta_{c,active}}{\theta_{c,passive}} \times 100\%$	47.59	58.26

3.3 Car Body Acceleration

Figures 13 to 15 show the lateral, yaw and roll accelerations responses of the railway car body with the same random inputs. From Figure 10 and Table 6, it can be found that the amplitude for lateral acceleration of the car body using active suspension is lower than that of using passive suspension with the percentage differences of 30.69 %. The passive suspension gave the value of 0.0596851 m/s^2 while active suspension was 0.0413657 m/s^2. The RMS values for the lateral acceleration were 0.01796 m/s^2 and 0.01546 m/s^2.

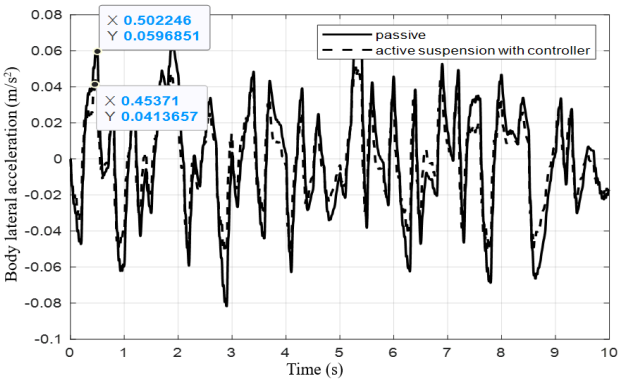

Figure 13 Railway body lateral acceleration response for random input disturbance

Table 6 Peak-to-peak and RMS values of body acceleration

Car body lateral acceleration	$\ddot{y}_c$ (m/s^2)	
	Peak to Peak	RMS
Passive suspension	0.0596851	0.01796
Active suspension (Modified skyhook controller)	0.0413657	0.01546
Improvement (%) $= \frac{\ddot{y}_{c,passive} - \ddot{y}_{c,active}}{\ddot{y}_{c,passive}} \times 100\%$	30.69	13.92

The percentage difference of body yaw acceleration (Figure 14) between the passive and active suspension is 60.90 % as shown in the Table 7. The value of high peaks for passive and active suspension with implementation of controller are 0.00424053 rad/s^2 and 0.00160677 rad/s^2 respectively. The RMS gave the reduction in amplitude with the percentage difference of 65.58 %.

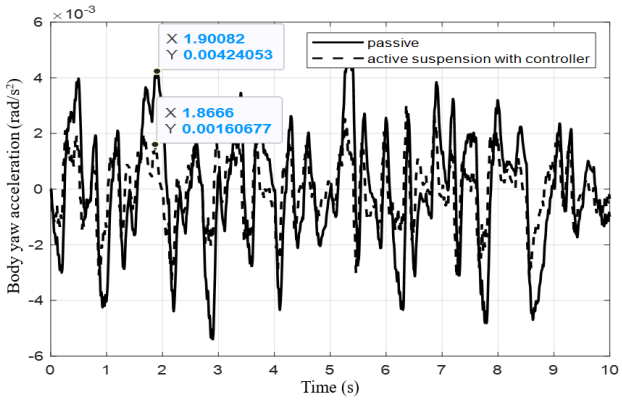

Figure 14 Railway body yaw acceleration response for random input disturbance

Table 7 Peak-to-peak and RMS values of body yaw acceleration for railway vehicles with different suspension systems

Car body yaw acceleration	$\ddot{\varphi}_c$ (rad/s^2)	
	Peak to Peak	RMS
Passive suspension	0.00424053	0.000991
Active suspension (Modified skyhook controller)	0.00160677	0.000344
Improvement (%) $= \frac{\ddot{\varphi}_{c,passive} - \ddot{\varphi}_{c,active}}{\ddot{\varphi}_{c,passive}} \times 100\%$	60.90	65.28

Figure 15 shows the results of body roll acceleration with different types of suspension where the value of peak-to-peak for the active suspension is lower than passive suspension due to the existing of modified controller that helps to reduce the acceleration of the car body. Table 8 tabulated the percentage difference of 30.55 % with the value of passive is 0.0261084 rad/s^2 and active suspension was 0.0181327 rad/s^2. The RMS improvement was 90.30 % with passive value of 0.002801 rad/s^2 and active value of 0.0002705 rad/s^2.

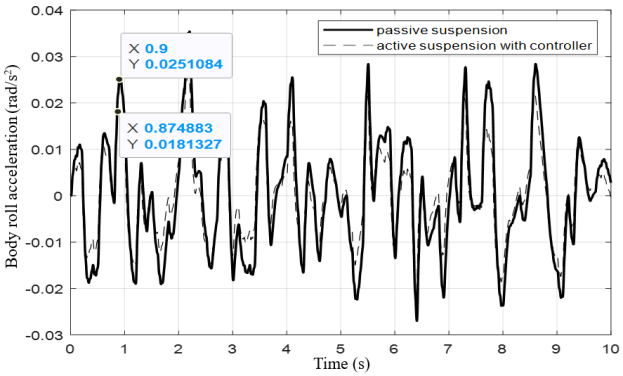

Figure 15 Railway body roll acceleration response for random input disturbance

Table 8 Peak-to-peak and RMS values of body roll acceleration for railway vehicles with different suspension systems (unit: lateral – rad/s²)

Car body roll acceleration	$\ddot{\theta}_c$(rad/s²)	
	Peak to Peak	RMS
Passive suspension	0.0261084	0.002801
Active suspension (modified skyhook controller)	0.0181327	0.0002705
Improvement (%) $= \frac{\ddot{\theta}_{c,passive} - \ddot{\theta}_{c,active}}{\ddot{\theta}_{c,passive}} \times 100\%$	30.55	90.30

Body accelerations and body displacements were both significantly reduced when the proposed controller was implemented. The modified skyhook controller shows a slight improvement and has the ability to significantly reduce unwanted body motions in response to random track irregularities input disturbances.

4.0 CONCLUSION

In this paper, a 13-DOF mathematical models of a full railway vehicle suspensions, including the car body, two bogies and four wheelsets, were developed and verified. The proposed modified skyhook controller played important roles at the secondary suspension system in reducing the vibrations. The random inputs at 0.01 m are considered as common track irregularities. The active secondary suspensions with proposed controller have suggestively reduced the car body lateral displacement and acceleration, yaw and roll angular displacements and accelerations at satisfactory percentages compared to the passive suspensions. These reductions in vibrations represent significant improvement in ride performance and ride quality of the railway vehicle. With available sensors, data logger, embedded electronic board and reliable actuators, the proposed controller can be implemented on the hardware-in-the-loop (HIL) for lab-scale experiment and actual railway vehicle for actual on field operation.

Conflicts of Interest

The author(s) declare(s) that there is no conflict of interest regarding the publication of this paper.

Acknowledgement

The authors gratefully acknowledge the support received from the Centre for Advanced Research on Energy (CARe) and the Universiti Teknikal Malaysia Melaka, Malacca, Malaysia under grant: PJP/2020/FKM/PP/S01784. This research is supported through the collaboration and MoU between Universiti Teknikal Malaysia Melaka (UTeM) and Universitas Sebelas Maret (UNS).

References

[1] Lee, S. Y., & Cheng, Y. C. 2005). Hunting Stability Analysis of High-speed Railway Vehicle Trucks on Tangent Tracks. *Journal of Sound and Vibration*. 282(3-5): 881-898.

[2] Habeeb, H. A., Mohan, A. E., Abdullah, M. A., Abdul, M. H., & Tunggal, D. 2020. Performance Analysis of Brake Discs in Trains. *Jurnal Tribologi*. 25: 1-15.

[3] Abdullah, M. A., Hassan, N. A., Foat, N. A. M., Shukri, M. F. A. M., & Mohan, A. E. 2018. Swaying Phenomenon of Express Railway Train in Malaysia. *Proceedings of Innovative Research and Industrial Dialogue*. 18: 98-99.

[4] Mohan, A. E., Abdullah, M. A., Azmi, M. A. I., Arsaat, A., Abdullah, W. M. Z. W., Harun, M. H., & Ahmad, F. 2018. Comfort Parameters Tuning Analysis for Vehicle Suspension Pitch Performance. *International Journal of Engineering and Technology (IJET)*. 9(6): 4471-4480.

[5] Ibrahim, M., Abdullah, M. A., Jamil, F. M., Harun, M. H., & Ahmad, F. 2017. Verification of Commercial Vehicle Ride Dynamics. *Proceedings of Innovative Research and Industrial Dialogue*. 16: 185-186.

[6] Kumar S.,Kumar A. 2017. Ride Comfort of a Higher Speed Rail Vehicle using a Magnetorheological Suspension System. *Proc IMechE Part K: J Multi-body Dynamics*. Doi: 10.1177/1464419317706873.

[7] Abdullah, M. A., Ridzuan, M. R., Ahmad, F., Jamil, F. M., & Ibrahim, M. 2017. Vehicle Active Suspension Control using Multi-order PID Approach. *Journal of Advanced Manufacturing Technology (JAMT)*. 11(1): 1-14.

[8] Zong, L.H., Gong, X. L., Xuan, S. H. and Guo, C. Y. 2013. Semi-active H∞ Control of High-speed Railway Vehicle Suspension with Megnetoheological Dampers. Vehicle System Dynamics. *International Journal of Vehicle Mechanics and Mobility*. 51(5): 600-626. http://dx.doi.org/10.1080/00423114.2012.758858.

[9] Dong, X., Yu, M., Liao, C., *et al*. 2010. Comparative Research on Semi-active Control Strategies for Magneto-Rheological Suspension. *Nonlinear Dynamics*. 59(3): 433-453. Doi 10.1007/s11071-009-9550-8.

[10] Goncalves, F. D. 2001. Dynamic Analysis of Semi-active Control Techniques for Vehicle Applications. Virginia Polytechnic Institute and State University. 1.

[11] Yagiz, N., Gursel, A. 2005. Active Suspension Control of a Railway Vehicle with a Flexible Body. *International Journal*

of Vehicle Autonomous Systems. 3(1): 80-95. Doi: 10.1504/ijvas.2005.007039.
[12] Sam, Y. M., Osman, J. H. S., Ghani, M. R. A. 2012. Sliding Mode Control of Active Suspension System. *Jurnal Teknologi.* 37(D): 1-10. Doi: https://doi.org/10.11113/jt.v37.534.
[13] Al-Zughaibi A., Davies H. 2015. Controller Design for Active Suspension System of ¼ Car with Unknown Mass and Time-Delay. *International Journal of Mechanical, Aerospace, Industrial, Mechatronic and Manufacturing Engineering*. 9(8).
[14] Selamat, H., & Zawawi, M. A. 2009. Active Control of High-Speed Railway Vehicles. *Elektrika*. 11(1): 1-7.
[15] Abdullah, M. A., Jamil, J. F., Mohamad, M. A., Rosdi, R. S., Ramlan, M. N. I. 2015. Design Selection and Analysis of Energy Regenerative Suspension. *Jurnal Teknologi*. 76(10): 27-3. Doi: https://doi.org/10.11113/jt.v76.5789.
[16] Jamil, J. F., Abdullah, M. A., Tamaldin, N., & Mohan, A. E. 2015. Fabrication and Testing of Electromagnetic Energy Regenerative Suspension System. *Jurnal Teknologi*. 77(21).
[17] Kim, C., Ro, P. I. 1997. A Sliding Mode Controller for Vehicle Active Suspension Systems with Non-linearities. *Journal of Automobile Engineering.* 212.
[18] Nor, A. S. M, Selamat, H., Alimin, A. J. 2011. Optimal Controller Design for A Railway Vehicle Suspension System Using Particle Swarm Optimization. *Jurnal Teknologi.* 54: 71-84. Doi: https://doi.org/10.11113/jt.v54.92.
[19] Shin, Y. J., You, W. H., Hur, H. M., & Park, J. H. 2014. H∞ Control of Railway Vehicle Suspension with MR Damper using Scaled Roller Rig. *Smart Materials and Structures.* 23(9). https://doi.org/10.1088/0964-1726/23/9/095023.
[20] Gopala Rao, L. V. V., Narayanan, S. 2009. Sky-hook Control of Nonlinear Quarter Car Model Traversing Rough Road Matching Performance of LQR Control. *Journal of Sound and Vibration.* 323(3-5): 515-529. https://doi.org/10.1016/j.jsv.2009.01.025.
[21] Yang, J., Li, J., Du, Y. 2006. Adaptive Fuzzy Control of Lateral Semi-active Suspension for High-Speed Railway Vehicle. *International Conference on Intelligent Computing*. 1104-1115.
[22] Yang, Z., Zhang, J., Chen, Z., Zhang, B. 2011. Semi-active Control of High-speed Trains Based on Fuzzy PID Control. *Proceedia Engineering.* 15: 521-525. Doi: 10.1016/j.proeng.2011.08.099.
[23] Chen, Y. 2009. Skyhook Surface Sliding Mode Control on Semi-active Vehicle Suspension Systems for Ride Comfort Enhancement. *Engineering.* 1(1): 23-32.
[24] Yamin, A. H. M., Talib, M. H. A., Darus, I. Z. M., Nor, N. S. M. 2022. Magneto-Rheological (MR) Damper – Parametric Modelling and Experimental Validation for Lord RD 8040-1. *Jurnal Teknologi.* 84(22): 27-34.
[25] Bhardawaj, S., Sharma, R. C., & Sharma, S. K. 2020. Development of Multibody Dynamical using MR Damper based Semi-active Bio-inspired Chaotic Fruit Fly and Fuzzy Logic Hybrid Suspension Control for Rail Vehicle System. *Proceedings of the Institution of Mechanical Engineers, Part K: Journal of Multi-Body Dynamics.* 234(4): 723-744. https://doi.org/10.1177/1464419320953685.
[26] Wang, D. H., Liao, W. H. 2009. Semi-active Suspension Systems for Railway Vehicles using Magnetorheological Dampers. Part I: System Integration and Modelling. *Vehicle System Dynamics.* 47(11): 1305-1325. Doi: 10.1080/00423110802538328.
[27] Harun, M. H., Abdullah, M. A., Abu Bakar, S. A., Mohammad Nasir, M. Z., W. Abdullah, W. M. Z., & Wan Mohamad, W. M. F. 2020. Railway Vehicle Stability Improvement using Bogie-based Skyhook Control. *Proceedings of Mechanical Engineering Research Day*. 2020: 41-42.
[28] Harun, M. H., Abdullah, W. M. Z. W., Jamaluddin, H., Rahman, R. A., & Hudha, K. 2014. Hybrid Skyhook-stability Augmentation System for Ride Quality Improvement of Railway Vehicle. *Applied Mechanics and Materials.* 663: 141-145. https://doi.org/10.4028/www.scientific.net/AMM.663.141.
[29] Jamil, F. M., Harun, M. H., Abdullah, M. A., Ibrahim, M., & Ahmad, F. 2022. Railway Car Body Lateral Hunting Attenuation using Body-based Modified Skyhook Control for Secondary Suspension. *Proceedings of Mechanical Engineering Research Day*. 2022: 234-235.
[30] Bakar, S. A. A, Jamaluddin, H. Rahman, R. A., Samin, P. M. Hudha, K. 2008. Vehicle Ride Performance with Semi-active Suspension System using Modified Skyhook Algorithm and Current Generator Model. *International Journal of Vehicle Autonomous Systems.* 6(3/4): 197-221. Doi:10.1504/ijvas.2008.023577.
[31] Karnopp, D., Crosby, M. J., and Harwood, R. A. 1974. Vibration Control using Semi-active Force Generators. *Journal of Engineering for Industry*. 96: 619-626.
[32] Abulifa, A. A., Ahmad, R. R., Soh, A. C., Radzi, M. A. M., & Hassan, M. K. 2017. Modelling and Simulation of Battery Electric Vehicle by using MATLAB-Simulink. *2017 IEEE 15th Student Conference on Research and Development (SCOReD)* IEEE. 383-387.